Effect of Mutation on the Dissociation and Recombination Dynamics of CO in Transcriptional Regulator CooA: A Picosecond Infrared Transient Absorption Study†

Tieqiao Zhang,*,‡ Igor V. Rubtsov,§ Hiroshi Nakajima,|| Shigetoshi Aono,⊥ and Keitaro Yoshihara*,@

School of Materials Science, Japan Advanced Institute of Science and Technology, Tatsunokuchi, Ishikawa 923-1292, Japan

Received February 21, 2006; Revised Manuscript Received May 25, 2006

ABSTRACT: The CO ligation process in a mutant (H77G) of CooA, the CO-sensing transcriptional regulator in *Rhodospirillum rubrum*, is studied with femtosecond time-resolved transient absorption spectroscopy in the mid-infrared region. Following photolyzing excitation, a transient bleach in the vibrational region of bound CO due to the CO photodissociation is detected. In contrast to the spectra of the wild-type (WT) CooA, the transient bleach spectra of H77G CooA show a bimodal shape with peaks shifting to the lower frequency during spectral evolution. The CO recombination dynamics show single-exponential behavior, and the CO escaping yield is higher than that of the WT CooA. A reorientation process of CO relative to the heme plane during recombination is revealed by anisotropy measurements. These phenomena indicate changes in the protein response to the CO ligation and suggest an alteration to the CO environment caused by the mutation. On the basis of these results, the role of His77 in the CO-dependent activation of CooA and a possible activation mechanism involving collaborative movement of the heme and the amino residues at both sides of the heme plane are discussed.

Heme proteins make up an important category of proteins in biology known for their special feature of ligand−heme interaction. Due to this feature, they perform a wide variety of functions in biology, such as oxygen storage and/or transport, electron transfer, and redox catalysis with various substrates (*1*). Other than these well-known functions, recently, new roles as sensors and/or transcriptional regulators have been found upon discovery of some new heme proteins (*2*−*6*). Similar to their well-known relatives, these new heme proteins perform their sensor functions depending on the ligation of effectors to the heme group. However, emerging with the new functions, these new heme proteins also exhibit new characteristics in the ligation of effectors to the heme group.

One of these heme proteins is CooA,[1] a sensor protein found in a photosynthetic bacterium *Rhodospirillum rubrum*. *R. rubrum* can grow on CO as the sole energy source (*7*). The utilization of CO depends on the expression of the *coo* operons, for which CooA works as a transcriptional regulator (*8*). CooA is also the sensor protein specific to CO in *R. rubrum*. It is the first known CO-sensing heme protein; therefore, its CO sensing and activation mechanisms have attracted serious attention from researchers since its discovery.

CooA is an ∼50 kDa homodimer with each subunit having a *b*-type heme as the prosthetic group (*8*, *9*). It belongs to a superfamily of transcriptional activator proteins that includes the cyclic AMP (cAMP) receptor protein (CRP) and the fumarate and nitrate reductase activator protein (FNR) (*10*). So far, only the crystal structure of CooA without the effector (CO) is available. The crystal structure of the CooA−CO complex has not yet been obtained, so the activation mechanism of CooA is still not clear. Fortunately, the crystal structure of CRP with the effector (cAMP) has been available. From the analogy of the two proteins, a scheme for the activation of CooA has been proposed. Upon ligation of CO to the heme, CooA changes its conformation significantly, from the nonactive "off" state to the DNA binding "on" state, and binds to the target DNA to initiate gene expression (*11*−*13*). Nevertheless, a detailed activation mechanism is still lacking. Therefore, it is necessary to study the ligation process in these heme proteins.

Although how CooA changes its conformation upon activation is not completely understood, studies have revealed that several unique ligand exchange processes play key roles

† This work is supported in part by the Grant-in-Aid Program for Scientific Research (11554028, 12680631, 12147203, and 14380303) of the Ministry of Education, Culture, Sports, Science and Technology of Japan and a Grant-in-Aid for JSPS Fellow (P00125) from the Japan Society for the Promotion of Science.

* To whom correspondence should be addressed. T.Z.: telephone, (301) 402-5722; fax, (301) 496-9933; e-mail, zhangti@mail.nih.gov. K.Y.: telephone and fax, +81-561-63-6918; e-mail, Riken-Yoshihara@mosk.tytlabs.co.jp.

‡ Present address: Imaging Science Program, Clinic Center, National Institutes of Health, Bethesda, MD 20892.

§ Present address: Department of Chemistry, Tulane University, New Orleans, LA 70118.

|| Present address: Department of Chemistry, Graduate School of Science, Nagoya University, Furo, Chikusa, Nagoya 464-8602, Japan.

⊥ Present address: Okazaki Institute for Integrative Bioscience, National Institutes of Natural Sciences, 5-1 Higashiyama, Myodaiji, Okazaki, Aichi 444-8787, Japan.

@ Present address: Toyota Physical and Chemical Research Institute, Nagakute, Aichi 480-1192, Japan.

[1] Abbreviations: CO, carbon monoxide; WT, wild type; CooA, carbon monoxide oxidation activator.

10.1021/bi0603672 CCC: $33.50
Published on Web 07/04/2006

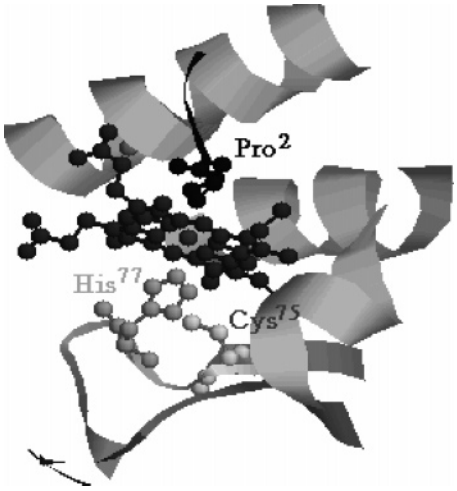

FIGURE 1: Schematic view of the heme environment and the locations of several key amino acid residues relative to the heme in non-CO binding WT CooA (*15*) (Protein Data Bank entry 1ft9). CooA is a homodimer protein; the heme and His77 in the graph belong to a same subunit, while Pro2 is from the other subunit.

in the activation. The heme groups of CooA have a very unique coordination structure (see Figure 1 for the protein structure around the heme). It always has two axial ligands; i.e., it is always six-coordinate. The first axial ligand exchange takes place between Cys75 and His77, accompanying the change in the oxidation state of the heme iron (*12*, *14*). Cys75 is the proximal ligand of the ferric heme, which is replaced with His77 upon reduction of the heme iron, and vice versa. Second, Pro2 is the distal ligand of the ferric and ferrous hemes in CooA before CO binding (*15*−*17*). It is the first example of proline being a heme ligand. CO reacts with the ferrous heme under physiological conditions to form the CO-bound heme (*8*, *9*, *12*). Since the heme already has two axial ligands before CO binding, CO must replace one of the axial amino ligands. EXAFS and NMR spectroscopies reveal that it is Pro2 that is replaced with CO upon CO binding (*16*, *17*). The ligand exchange processes and the drastic difference between the conformations of the protein in on and off states (*15*) reveal a flexible protein matrix, different from other heme proteins, including myoglobin. These unique features further intrigued researchers.

Because the crystal structure of the CooA−CO complex is still lacking, spectroscopy methods have been found to be especially useful in revealing the dynamics of CO ligation and the protein conformational change (*17*−*21*). In the resonance Raman study, Uchida et al. (*21*) found that the presence of the target DNA slows the recombination of photodissociated CO in the millisecond time range. Our studies by femtosecond time-resolved UV−vis and IR spectroscopy revealed that a large proportion of photodissociated CO (>90%) geminately recombined with the heme in less than 1 ns in the absence of the target DNA (*18*, *19*). Furthermore, in the IR study, we observed a peak shift in the transient absorption spectra of the bound CO with a time constant of ∼160 ps and attributed it to a conformational change of the protein following CO dissociation (*19*).

So far, the function of the distal side heme environment has been explored well. The ligand exchange between Pro2 and CO was once thought to be the most crucial process for the activation of CooA as a gene transcriptional activator because only the CO-bound form of CooA can bind to its target DNA (*11*−*13*, *22*). It was suggested that the move of the amino-terminal polypeptide chain induced by releasing Pro2 from the heme by CO caused the activation of CooA. However, recent studies showed that the CO-dependent CooA activation mechanism is not so simple. The amino acid residues at the proximal side, including His77, may even play some unidentified but important role in the CO-dependent activation of CooA (*14*). To understand the protein response to the CO ligation comprehensively, the function of the proximal side heme environment needs to be addressed. Especially, the obviously important but hitherto obscure role of His77 in the activation needs to be revealed. For this purpose, we investigated the CO recombination dynamics in a CooA His77 mutant, H77G, with femtosecond time-resolved mid-IR transient absorption spectroscopy. The results reveal a conformational alteration by the mutation and indicate the function of an amino acid residue at the proximal side that maintains the correct protein conformation for activation. His77 is suggested to work as a tethering supporter for the heme. A cooperative model for the CooA activation involving all the parts that make up the CO environment, i.e., the heme and the amino acid residues around the heme, was proposed.

MATERIALS AND METHODS

H77G CooA, in which His77 is replaced with Gly, was obtained by site-directed mutagenesis (*12*). Procedures for expression and purification have been described previously (*9*, *12*). After preparation, the mutant was reduced and bound with CO anaerobically in Tris/boric acid buffer in D_2O at pH 8, as in the case of WT CooA (*19*). The final heme concentration of the sample was ∼1 mM. Under a nitrogen atmosphere, the sample was added to a sample cell that was made of two 1 mm thick CaF_2 windows separated by a 0.2 mm Teflon spacer.

The femtosecond time-resolved UV−visible pump mid-IR probe spectrometer has been described elsewhere (*19*, *23*). Briefly, mid-IR pulses at ∼5 μm were generated at 1 kHz by the difference frequency generation of the signal and idler pulses from an OPA. The bandwidth of the mid-IR pulses was ∼150 cm^{-1}. The mid-IR beam was divided into two parts, the probe and the reference. The probe beam was focused onto a sample cell with a CaF_2 lens with a focal length of 12 cm, yielding a spot size of ∼120 μm. The second harmonic (400 nm) of the residual fundamental from the OPA was used as the excitation pulse. The excitation pulses passed a mechanical chopper working at half of the repetition rate of the laser pulses, a variable delay line, a variable neutral-density filter, and a half-wave plate before being focused onto the sample cell by a lens with a focal length of 17 cm. The spot size of the pump beam on the sample cell was ∼150 μm. Finally, the probe and the reference mid-IR beams were focused into a monochromator, in which the two beams were separated and sent to two mercury cadmium telluride detectors. The spectral resolution was 3.6 cm^{-1}. The instrument response function was estimated to be less than 250 fs (fwhm) by measurement of the electronic response of a thin silicon plate at the sample position. The anisotropy measurements were made by rotating the polarization of the pump beam with the half-wave plate. The anisotropy data were constructed from scans with the polarization of the

pump beam alternating between parallel to and perpendicular to the polarization of the probe beam.

The sample cell was kept constantly spinning to provide fresh sample for each pulse. A flow of cooled nitrogen was used to keep the sample at ~5 °C during the experiment. The excitation power was reduced to ~0.3−0.4 μJ/pulse, producing ~20% excitation of the sample. No obvious degradation of the sample was observed after the experiments from comparison of the steady-state absorption spectra before and after the experiment.

RESULTS

CO Geminate Recombination. Photoexcitation of the heme at its Soret band causes the dissociation of the ligated CO, which produces a negative change in the absorption of the bound CO (a bleach signal). The rebinding of the CO molecule to the heme causes the bleach signal to decay. As in the case of WT CooA (*19*), decay dynamics of the bleach signal vary with the wavelength of observation.

Reconstructed time-resolved spectra were fitted well with two Gaussian components (discussed below). Global fitting therefore has been utilized to fit spectra and dynamics simultaneously (*24*). At the peak position of the bleach signal (1972 cm^{-1}), the decay dynamics that are associated with the main Gaussian component are fitted with a single-exponential function with a time constant of 80 ± 3 ps and a persisting component with an amplitude close to 50%. It has been shown that the bimolecular binding of CO from solution to the heme of the CooA is a very slow process with a rate constant of ~10 μM^{-1} s^{-1} (*21*). As a result, if CO escapes from the heme pocket, the rebinding time is on the order of milliseconds. This slow process appears as a constant in our observation time window (*19*, *23*). Therefore, we attribute the fast 80 ps decaying component to the geminate recombination process and the persisting component to the escape of CO from the heme environment.

The CO rebinding dynamics of the mutant differ from those of WT CooA, Mb, or Hb (Figure 2a). In Figure 2a, the normalized decay dynamics at the maximum bleach wavelength for both WT CooA (1977 cm^{-1}) and the mutant (1972 cm^{-1}) are shown for comparison. In the case of WT CooA, the decay dynamics were nonexponential and fitted well with a two-exponential decay function with time constants of 56 ± 7 ps (55%) and 290 ± 40 ps (43%) (*19*). A persisting component accounts for only 2% of the total bleach. So in our previous study of WT CooA, the vast majority of the photolyzed CO rebinds geminately and only a small proportion escapes (*19*). A tight heme pocket has been inferred from the much faster geminate recombination rate and the much higher geminate recombination yield compared with those of Mb and Hb (*19*) (for detailed discussions on the WT CooA protein, see ref *19*). On the other hand, the dynamics of CO−heme recombination in Mb show just a nondecaying flat line in our experiments due to a much slower recombination rate with a much lower recombination yield (~4%) (see Figure 1 of the Supporting Information). However, the dynamics in H77G CooA are intermediate between the dynamics of WT CooA and Mb. While there is still fast geminate recombination, the persisting part increases to ~50%. These unique dynamics suggest a CO environment that differs from those of WT CooA, Mb, or Hb. Especially, the drastically increased yield of CO escaping from the heme pocket indicates an alteration to the protein structure of CooA by the mutation (see the Discussion).

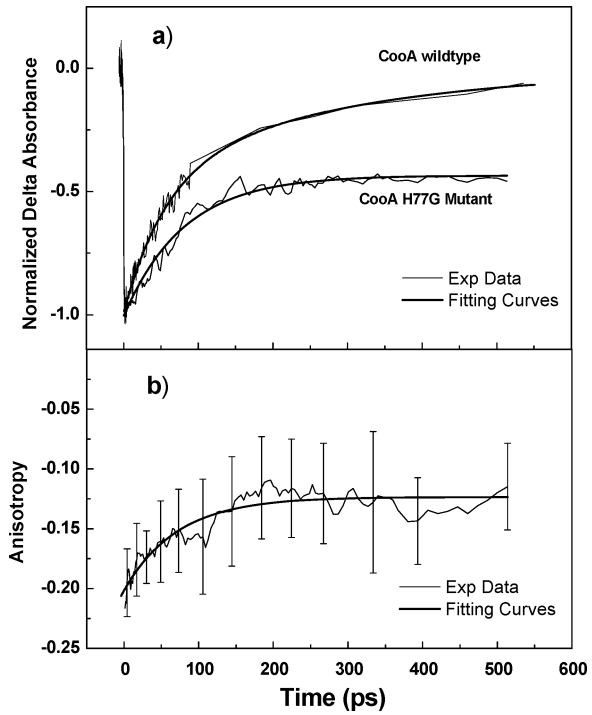

FIGURE 2: (a) Normalized decay dynamics at wavelengths of the maximums of the transient bleach spectra of WT CooA (1977 cm^{-1}) and H77G CooA (1972 cm^{-1}). For H77G CooA, the curve shows decay at the magic angle reconstructed from data of perpendicular and parallel measurements. For WT CooA, the data were collected under the perpendicular condition since there is no anisotropy change. Thick lines are fitting curves as described in the text. (b) Anisotropy change over time for H77G CooA obtained from the data of perpendicular and parallel measurements as described in the text. The error bars at some points show a typical noise level.

Anisotropy Dynamics of the Rebound CO. The time-resolved anisotropy of the C−O stretching mode at 1972 cm^{-1} is shown in Figure 2b. Clearly, there is an increase in the anisotropy value in the first 200 ps. This observation contrasts with our previous experiment on WT CooA for which no time-dependent anisotropy change was observed (*19*). This suggests that in the mutant the favorable orientation for the rebinding of CO to the heme is different from the original orientation during the CO rebinding process (see the Discussion).

Calculations provide more details about the change in the CO rebinding orientation. In our model, the heme is regarded as a circular absorber for the excitation at 400 nm with the transition moment in the porphyrin plane, and the transition moment of the C−O stretch vibration is treated as being along the C−O line (*19*). Under the conditions described above, the relation $r(\varphi) = 0.1(3\cos^2\varphi - 2)$ is deduced, where φ is the angle between the porphyrin plane and the CO line and $r(\varphi)$ the corresponding anisotropy value deduced from raw data with considering the photolysis level and the sample thickness (for procedures for correcting the raw anisotropy data, see refs 46 and 47 of ref *19* and the footnotes in ref *19*). By using this equation, calculation shows that the angle φ is 86 ± 3° just after the photolysis while it gradually changes to ~63° after 200 ps. (The reliability of

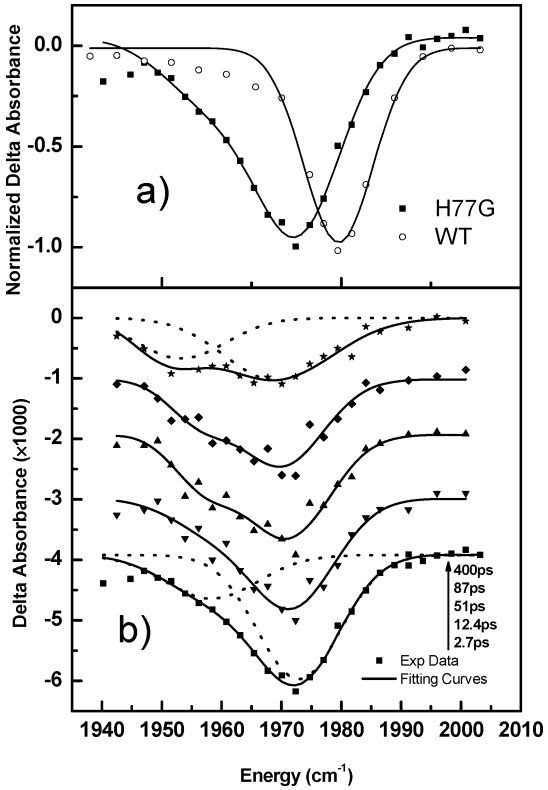

FIGURE 3: (a) Transient bleach IR absorption spectra in the bound CO stretching region of WT CooA 1.4 ps and H77G CooA 2.7 ps after photoexcitation. (b) Transient bleach IR absorption spectra in the bound CO stretching region of H77G CooA on different delay times after photoexcitation. Spectra are shifted vertically for clarity. The solid lines are fitting curves generated with a sum of two Gaussian components that are shown as dotted lines.

the results and data processing procedures was proven by experiment on CO-bound Mb under the same experimental conditions. See the Supporting Information.) An exponential fitting to the anisotropy change results in a time constant of 71 ± 6 ps. This time constant is close to the time constant of decay dynamics of the bleach signal, suggesting a close relation between them.

Evolution of Transient Spectra. The transient absorption difference spectrum of the mutant in D_2O in the region of the stretching vibration of the bound CO measured on a 2.7 ps time delay after the photoexcitation of the heme is shown in Figure 3a. The corresponding spectrum of the WT CooA−CO complex is also shown for comparison. The spectrum of the mutant is obviously broader than that of WT CooA, which exhibits a single peak (for details of the spectrum of WT CooA, see ref *19*). The spectral width of the WT CooA−CO complex spectrum is ∼14 cm^{-1} (fwhm), similar to that of the Mb−CO complex (12.5 cm^{-1} in ref *19* and 13 cm^{-1} in ref *25*). In the case of the H77G mutant, the spectrum is much broader (fwhm ∼ 19 cm^{-1}) and an asymmetry of the two wings of the spectrum suggests the existence of two peaks, which becomes more apparent at later delay times.

The spectra at different delay times are shown in Figure 3b. The solid lines are fitting curves generated with a sum of two Gaussian functions (showed as dotted lines). At the beginning, the stronger Gaussian component has a central frequency of 1972 cm^{-1} while the weaker one, which is more prominent at a later time, has a central frequency of ∼1958 cm^{-1}. The widths of the peaks are both ∼15 cm^{-1} (fwhm),

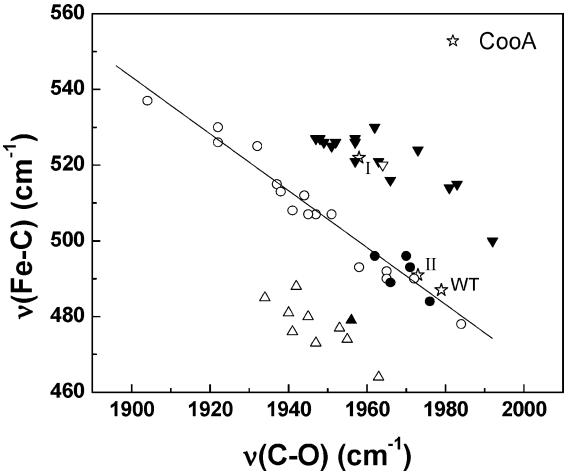

FIGURE 4: Relation between the C−O stretching frequency and the Fe−C stretching frequency of heme−CO adducts (data from refs *30*−*33*). Filled symbols are for model chemical systems. Empty symbols are for proteins. The line stands for the linear fitting for hexaligated hemes with neutral imidazole as the axial ligand trans to CO (○ and ●). The top group (▽ and ▼) is pentaligated hemes, and the bottom group (△ and ▲) is hexaligated hemes with thiolate as the trans ligand. WT CooA and H77G CooA are shown as empty stars labeled WT, I, and II (see the text), respectively.

which is close to the separation between them, ∼14 cm^{-1}. By comparing those spectra, we find it is clear that the two contributions decay with different rates (see the Discussion for details). As shown in Figure 2a, the bleach signal at 1972 cm^{-1} decays with a time constant of 80 ± 3 ps. The time constant is 97 ps for the decay of the bleach signal at 1958 cm^{-1} (data not shown). The signals at 1972 and 1958 cm^{-1} are assigned to six- and five-coordinate CO-bound species, respectively (see the Discussion for details).

In the bleach spectra of the WT CooA−CO complex, a biexponential peak shift to the lower frequency was observed (*19*). A characteristic time of ∼160 ps was obtained from the weighted average of the two time constants, which is almost equal to the average geminate recombination time (155 ps). In the transient spectra of the mutant, the red shift of the peaks was observed for both bands, though the corresponding characteristic times are different. The peak shift of the main band at 1972 cm^{-1} can be fitted well with an exponential function. The characteristic time of the spectral shift (79 ps) coincides with the time constant of the decay dynamics (80 ps) and is close to the time constant of the anisotropy change (71 ps), suggesting a close relation among the time constants. The characteristic time for the peak shift of the other band at 1958 cm^{-1} is 131 ps. Both time constants are shorter than that of the wild-type protein (160 ps).

DISCUSSION

Assignment of Transient Spectra and Coordination Structure. Studies on heme proteins and heme complexes have proven a negative linear relation between the Fe−C and C−O stretching frequencies as illustrated in Figure 4 (*26*−*32*). This phenomenon has been explained with a back-donation model in which the electron donation between the iron and CO is affected by the electrostatic field around the heme−CO environment (*27*−*30*). Thus, the relation of the Fe−C and C−O frequencies can be regarded as an indicator of the heme coordination structure (*31*).

However, the electron donation is also affected by the trans ligand (the other axial ligand of the heme opposite from the CO molecule), known as the trans effect (*26*, *30*). In Figure 4, the data could clearly be classified into three groups, according to the electron donating strength of the trans ligands: (1) the middle group of globins and model systems with a neutral imidazole (including histidine) as the trans ligand, (2) the lower group of proteins or systems with stronger σ-donating trans ligands such as thiolate or imidazolate, and (3) the upper group that includes hemes with weaker σ-donating trans ligands, and five ligated hemes. The point for WT CooA (white star) is located very close to the imidazole line, consistent with the fact that His77 is the proximal ligand, i.e., the trans ligand (*15*, *20*).

For H77G CooA, two peaks are observed at 1973 and 1958 cm^{-1} for the stretching mode of the heme-bound CO in our study, as shown in Figure 3b. Two Fe−CO stretching modes are observed at 491 and 522 cm^{-1} in the resonance Raman spectrum of the CO-bound H77G CooA, which are assigned to six- and five-coordinate species, respectively (*33*). From the linearity of the Fe−C and C−O frequencies, we associate the Fe−C and C−O frequencies in the following way (*34*), i.e., 522 and 1958 cm^{-1} with point I and 491 and 1973 cm^{-1} with point II (Figure 4). From this assignment, two conclusions can be drawn. First, point I clearly belongs to the pentaligated group, so the band at 1958 cm^{-1} is assigned to the C−O stretching mode of a five-coordinate (5-c) CooA−CO complex. Because the heme of H77G CooA in the reduced form still contains Pro2 as the distal ligand, the finding that CO is the only axial ligand in this 5-c species suggests that CO still ligates at the distal side, replacing Pro2. Second, point II stands for a six-coordinate (6-c) heme species. The closeness of this point to the line of hemes with neutral imidazole as the trans ligand suggests that in this species the trans ligand has a donor ability similar to that of neutral imidazole. It has been suggested that Cys75 is the trans ligand in the ferrous-state H77G CooA (*16*). The side chain of Cys75 in H77G CooA might be a thiol instead of a thiolate because ferrous and CO-bound H77G CooA show the Soret peak at ca. 420 nm instead of 450 nm (*12*). In terms of back-donation ability, thioethers have the same ligand donor ability as imidazole and neutral cysteines have been shown to have the same donating strength as histidine (*32*). Therefore, Cys75 could be the trans ligand in the 6-c species. On the other hand, the difference in the donor abilities of Pro2 and neutral imidazoles rules out the possibility of Pro2 being the trans ligand. Therefore, it is highly probable that CO also binds the heme at the distal side for the 6-c species, with Cys75 being the trans ligand.

It is worth noting that in all spectra, including the resonance Raman, UV−vis absorption, steady-state, and time-resolved IR spectra, the 6-c species has a stronger intensity than the 5-c species, though the ratio between the contributions varies. On the grounds of the ratios, by assuming that the cross sections of the 5-c and 6-c species are similar in all measurements, we estimate that the proportion of 6-c species is ~60−80%. Therefore, in H77G CooA, the 6-c species is dominant, and we will mainly concentrate on it in the following discussions.

Transformation Process following the Photolysis in H77G CooA. The experimental results have shown that the frequency of the maximum of the transient absorption and the anisotropy are changing with time. Since the time constants of both processes are close to each other and both processes are sensitive to the protein conformations, we suggest a transient conformational change as the response of the mutant to the CO dissociation. In our previous study of WT CooA, a transient conformational change model has also been proposed. For WT CooA, it is found that the characteristic time of the spectral peak shift (160 ps) is very close to the average recombination time (155 ps, calculated as a weighted average of the two decay components). On the basis of that, a dynamical conformation change model that associates the decay dynamics with the peak shift in the transient absorption spectra has been proposed (*19*). Meanwhile, we also considered the possibility that CO recombines from multiple docking sites in the protein, resulting in nonexponential decay dynamics. In the second case, the peak shift in the transient absorption spectra would be independent of recombination dynamics. In the context in which the CO environment is altered by the mutation (as shown by the difference in the frequencies of bound C−O and Fe−C stretching mode), it is interesting to investigate the response of the protein to the photodissociation of CO under such conditions. In this study of the mutant, the time constant for the CO geminate recombination (80 ps) perfectly matches the time constant of the spectral evolution of the transient bleach (79 ps) and is also very close to the time constant of the anisotropy change. The re-occurrence of the coincidence among the time constants further supports the transient conformational change model. Therefore, we suggest a transient conformational change occurs as the CO dissociates from the heme, changing the electrostatic potential around the heme and affecting the CO rebinding rate and frequency.

Albeit, the multiple-docking site model is still possible. This model was originally proposed for Mb. However, until now, no unanimous conclusion about whether CO does become docked somewhere after photolysis in Mb could be reached (*35*−*37*). So this model is under debate even for Mb. Furthermore, it is worth noting that there are indeed large differences in many aspects of CooA and Mb, particularly the CO recombination dynamics and the immediate protein structure around the heme (for details on the difference between Mb and CooA, see the last section of the Discussion). Even if there are indeed docking sites in Mb for CO, the complicated situation prevents us from making a solid conclusion about the existence of multiple docking sites in CooA, but the matching between the time constants of spectral shift and decay dynamics does not support this model because it contradicts one base assumption of the multiple-docking site model, that the spectral evolution and the recombination dynamics are independent of each other.

There is a third explanation for the spectral evolution and the CO rebinding dynamics, which involves the re-establishment process of the equilibrium between the different preexisting CooA conformations (the inhomogeneity of CooA) and/or the kinetic hole burning effect. However, even though we could not completely rule out these possibilities, we think the likelihood of these possibilities is, in practice, very small for the following reasons. First, the experiment conditions in our experiments would not produce selective excitation of a (or some) particular conformation(s), which is a prerequisite for hole burning. Second, the time scale of

the dynamics does not match the usual time for a re-establishment process of the equilibrium between the different protein conformations. Third, until now, the effect of kinetic hole burning has been obvious only at low temperatures for CO−heme rebinding experiments (*38*, *39*). Forth, the frequency gap between substates is usually more than 10 cm^{-1}, while our spectral shift is only a few inverse centimeters. Furthermore, simulations with these models have been carried out but could not reproduce the experimental results. For the possibility of inhomogeneity of CooA, if there is broad distribution of CO orientations in equilibrium and the rebinding CO critically depends on the CO orientation, the inhomogeneity would also cause spectral shift and anisotropy change. However, until now, most X-ray crystallography studies have not shown a broad distribution of CO orientations. So this possibility is unlikely.

It is worth noting that in the recombination of CO to the heme after photolysis, the CO escaping yield drastically increases up to ~50% in H77G CooA compared with only 2% in WT CooA (*19*). It could be due to either a loss of control over photolyzed CO or a hindrance to the rebinding of photolyzed CO. As shown in Figure 2a, the biexponential recombination dynamics in WT CooA become single-exponential in H77G CooA, suggesting a loss of one process that promotes CO recombination in WT CooA. Therefore, we suggest that the transient conformational change initiated by the CO photodissociation in H77G CooA evolves in a way different from that in WT CooA. The conformational change following the CO photodissociation is advantageous for CO escape in H77G CooA, while it is the reverse in WT CooA.

The change in the CO orientation supports this idea. The anisotropy changes with time in H77G CooA, in contrast to being constant in WT CooA (*19*). According to the anisotropy measurements, the favorite orientation of rebinding of CO in H77G CooA is initially almost perpendicular to the heme plane, while later it gradually changes to ~27° tilted from the normal. The larger tilting angle of the rebinding CO with respect to the heme plane results in a reduction of the affinity of the iron ion for the rebinding CO and an increase in the yield of CO escape (*40*, *41*). Since in both cases, the wavelength of the anisotropy recorded corresponds to the 6-c heme, it rules out the possibility that the change in anisotropy is induced by a change in the coordination structure. Thus, the difference in the CO orientation dynamics reflects a dynamical alteration to the conformation of the protein around the binding site in H77G. All observations support the idea that there is a significant conformational alteration around the heme in H77G CooA after CO photodissociation. In contrast to that in WT CooA, the conformation alteration in H77G CooA helps CO escape. The change in conformation evolution illustrates the effects of the mutation and suggests the function of His77 as an important guide for CooA activation (see the next section).

As discussed above, there is a 5-c species whose C−O stretching frequency is lower than that of the 6-c form. Similar to the case of the 6-c species, the decay dynamics also show a single-exponential decay (measured time constant of 97 ± 28 ps), and the CO escaping yield (47%) is also higher than that of WT CooA. Therefore, a conformational alteration possibly occurs in the CO environment of the 5-c species like it does in the 6-c species.

Role of His77 in the Activation of CooA. Until recently, it had been thought that the replacement of Pro2 by CO is controlling the whole activation event (*12*, *14*, *17*). However, this event turns out to be not determinate for CooA activation (*42*). In the studies of CooA mutants, so far, complete loss of CO-dependent activation has been found with all mutants at His77 (*12*). In contrast, CO-dependent activation was not affected when Pro2 was mutated or deleted (*16*, *43*). This suggests an important role of His77 in the CO-dependent activation process of CooA. However, the mechanism of its involvement in the CO-dependent activation has not been known.

Since CooA is activated by the ligation of CO to the heme, the heme definitely plays a critical role. One should note that the heme in CooA is a *b*-type heme, which is not covalently bound to the apoprotein. This means that its position or orientation is more flexible than a *c*-type heme that is covalently attached. Lanzilotta et al. have proposed that the heme moves with respect to the protein matrix on reduction from the ferric to the ferrous state (*15*). A recent study by Youn et al. has suggested a heme movement toward the helix on CO binding (*44*). Therefore, the heme in CooA should not be regarded as a fixed entity, and its movement should be a key event for the activation. In this context, we suggest that His77 plays a crucial role for the CooA activation as a supporting tether for the heme (see Figure 1), like His170 in horseradish peroxidase (*45*). When His77 is mutated, the position and/or the orientation of the heme changes. The heme would drift and reorient more freely than in WT CooA. This perspective is consistent with our observation that the recombination dynamics, the spectral evolution, and the anisotropy change of the mutant are significantly different from those of WT CooA.

We suggest that cooperation involving the heme and the amino acids at the two sides of the heme is necessary for the correct conformational change for activation. In the activation process, not only the distal side residues but also the heme itself and the residues at the proximal side also play important roles. When CO binds to the heme of CooA, replacement of Pro2 with CO at the distal side makes the N-terminus released, providing a space for conformational changes. Correspondingly, a conformational change with repositioning of the heme group takes place and initiates the activation. During the activation process, His77 acts as a tether and supporter for the heme that limits and guides the movement of the heme, guaranteeing the conformational change proceeds in the correct way.

When His77 is mutated, the orientation and position of the heme may change as a result of losing the guidance and restriction of His77. Consequently, cooperation involving the heme and the amino acids at the two sides of the heme is lost. The conformational change develops in a way different from that in WT CooA. The correct conformation for DNA binding could not be achieved, resulting in the loss of activation for all His77 mutants.

Comparison with H93G Myoglobin. The dissociation and ligation process of CO in myoglobin (Mb) has been extensively studied. Therefore, it is interesting to compare this study of CooA with those on myoglobin, especially the H93G mutant of Mb, the counterpart to H77G CooA. In WT sperm whale Mb, the geminate CO−heme recombination is slow (time constant of ~4 μs) and the yield is low (~4%).

Replacing the proximal histidine with exogenous ligands [H93G(L)] results in an increase in the geminate recombination yield (from 4% in WT Mb to 85−96% in mutants depending on L) and faster recombination kinetics (a factor of 4−15 depending on L and solvent viscosity) (*46*−*48*). However, the CO geminate recombination yield in WT CooA is significantly high (∼98%), and the geminate recombination rate [$(160\ \text{ps})^{-1}$] is 4 orders of magnitude faster than that in WT sperm whale Mb [$(4\ \mu\text{s})^{-1}$] (*19*). Mutation of the proximal histidine causes a decrease in the CO geminate recombination yield (from 98 to 50%). All of these a strong contrast show that the CO recombination context in CooA differs drastically from that in Mb.

The differences could be explained with the difference in structures and biological functions of the two proteins. As discussed above, the CooA structure around heme is quite flexible. This flexibility is probably crucial for CooA's function as a transcriptional regulator, which undergoes significant conformational change upon activation. Consequently, the mutation at the proximal side (H77G) in CooA may significantly affect the local heme environment and even the overall protein conformation (including the distal side) through some correlations. But the distal side may not be so critical as His77, as proven by the fact that distal side mutants still function well.

As oxygen storage, Mb experiences a smaller overall protein conformation change upon CO binding. It has been proposed that the proximal ligand affects CO recombination in Mb mainly by changing the activation enthalpy through steric interactions and the proximal ligand plays a much less important role in determining the fate of dissociated CO in the distal pocket than the distal amino acids (*47*). Very recently, time-resolved X-ray crystallography has shown how the distal side amino acid residues control photodissociated CO (*37*). Interestingly, the X-ray crystallography also showed heme movement/reorientation on CO dissociation (*37*).

So, the importance of heme reposition and/or reorientation and the cooperation between the amino acids around the heme and the heme itself in controlling ligand binding or dissociation may be generally applicable to heme proteins. Just for different proteins, heme interacts more with a different side of it, therefore affecting the ligand binding dynamics differently.

CONCLUSIONS

The transient IR absorption of CO-bound H77G CooA is studied for the first time. The decay dynamics, spectral shifts, and anisotropy evolution over time are found to be significantly different from those of WT CooA. A conformational change is suggested to be the origin of the different dynamics. The heme is proposed to change its position and/or orientation with mutation. On the basis on these observations, a cooperative CooA activation scheme is proposed in which the involvement of the heme and the amino residues at both sides of the heme plane collaborate for the activation.

ACKNOWLEDGMENT

We thank Dr. Shigeichi Kumazaki for many helpful discussions. We also thank the reviewers for valuable comments.

SUPPORTING INFORMATION AVAILABLE

CO recombination dynamics in Mb in buffer solution. This material is available free of charge via the Internet at http://pubs.acs.org.

REFERENCES

1. Poulos, T. L., Cusanovich, M. A., Meyer, T. E., Tollin, G., Brunori, M., Antonini, G., Malatesta, F., Sarti, P., Wilson, M. T., Rifkind, J. M., and Webster, D. A. (1988) in *Heme Proteins* (Eichhorn, G. L., and Marzilli, L. G., Eds.) pp 1−271, Elsevier, New York.
2. Chan, M. K. (2001) Recent advances in heme-protein sensors, *Curr. Opin. Chem. Biol. 5*, 216−222.
3. Aono, S. (2003) Biochemical and biophysical properties of the CO-sensing transcriptional activator CooA, *Acc. Chem. Res. 36*, 825−831.
4. Aono, S., and Nakajima, H. (1999) Structure and function of CooA, a novel transcriptional regulator containing a b-type heme as a CO sensor, *Coord. Chem. Rev. 192*, 267−282.
5. Aono, S., and Nakajima, H. (2000) Transcriptional regulation of gene expression by metalloproteins, *Prog. React. Kinet. Mech. 25*, 65−107.
6. Gilles-Gonzalez, M. A., and Gonzalez, G. (2005) Heme-based sensors: Defining characteristics, recent developments, and regulatory hypotheses, *J. Inorg. Biochem. 99*, 1−22.
7. Kerby, R. L., Ludden, P. W., and Roberts, G. P. (1995) Carbon monoxide-dependent growth of rhodospirillum-rubrum, *J. Bacteriol. 177*, 2241−2244.
8. Shelver, D., Kerby, R. L., He, Y. P., and Roberts, G. P. (1997) CooA, a CO-sensing transcription factor from *Rhodospirillum rubrum*, is a CO-binding heme protein, *Proc. Natl. Acad. Sci. U.S.A. 94*, 11216−11220.
9. Aono, S., Nakajima, H., Saito, K., and Okada, M. (1996) A novel heme protein that acts as a carbon monoxide-dependent transcriptional activator in *Rhodospirillum rubrum*, *Biochem. Biophys. Res. Commun. 228*, 752−756.
10. Shelver, D., Kerby, R., He, Y., and Roberts, G. (1995) Carbon monoxide-induced activation of gene-expression in *Rhodospirillum rubrum* requires the product of CooA, a member of the cyclic-AMP receptor protein family of transcriptional regulators, *J. Bacteriol. 177*, 2157−2163.
11. Aono, S., Matsuo, T., Shimono, T., Ohkubo, K., Takasaki, H., and Nakajima, H. (1997) Single transduction in the transcriptional activator CooA containing a heme-based CO sensor: Isolation of a dominant positive mutant which is active as the transcriptional activator even in the absence of CO, *Biochem. Biophys. Res. Commun. 240*, 783−786.
12. Aono, S., Ohkubo, K., Matsuo, T., and Nakajima, H. (1998) Redox-controlled ligand exchange of the heme in the CO-sensing transcriptional activator CooA, *J. Biol. Chem. 273*, 25757−25764.
13. He, Y. P., Shelver, D., Kerby, R. L., and Roberts, G. P. (1996) Characterization of a CO-responsive transcriptional activator from *Rhodospirillum rubrum*, *J. Biol. Chem. 271*, 120−123.
14. Shelver, D., Thorsteinsson, M. V., Kerby, R. L., Chung, S. Y., Roberts, G. P., Reynolds, M. F., Parks, R. B., and Burstyn, J. N. (1999) Identification of two important heme site residues (cysteine 75 and histidine 77) in CooA, the CO-sensing transcription factor of *Rhodospirillum rubrum*, *Biochemistry 38*, 2669−2678.
15. Lanzilotta, W. N., Schuller, D. J., Thorsteinsson, M. V., Kerby, R. L., Roberts, G. P., and Poulos, T. L. (2000) Structure of the CO sensing transcription activator CooA, *Nat. Struct. Biol. 7*, 876−880.
16. Nakajima, H., Honma, Y., Tawara, T., Kato, T., Park, S. Y., Miyatake, H., Shiro, Y., and Aono, S. (2001) Redox properties and coordination structure of the heme in the CO-sensing transcriptional activator CooA, *J. Biol. Chem. 276*, 7055−7061.
17. Yamamoto, K., Ishikawa, H., Takahashi, S., Ishimori, K., Morishima, I., Nakajima, H., and Aono, S. (2001) Binding of CO at the pro(2) side is crucial for the activation of CO-sensing transcriptional activator CooA: ^{1}H NMR spectroscopic studies, *J. Biol. Chem. 276*, 11473−11476.
18. Kumazaki, S., Nakajima, H., Sakaguchi, T., Nakagawa, E., Shinohara, H., Yoshihara, K., and Aono, S. (2000) Dissociation and recombination between ligands and heme in a CO-sensing transcriptional activator CooA: A flash photolysis study, *J. Biol. Chem. 275*, 38378−38383.

19. Rubtsov, I. V., Zhang, T. Q., Nakajima, H., Aono, S., Rubtsov, G. I., Kumazaki, S., and Yoshihara, K. (2001) Conformational dynamics of the transcriptional regulator CooA protein studied by subpicosecond mid-infrared vibrational spectroscopy, *J. Am. Chem. Soc. 123*, 10056−10062.
20. Uchida, T., Ishikawa, H., Ishimori, K., Morishima, I., Nakajima, H., Aono, S., Mizutani, Y., and Kitagawa, T. (2000) Identification of histidine 77 as the axial heme ligand of carbonmonoxy CooA by picosecond time-resolved resonance Raman spectroscopy, *Biochemistry 39*, 12747−12752.
21. Uchida, T., Ishikawa, H., Takahashi, S., Ishimori, K., Morishima, I., Ohkubo, K., Nakajima, H., and Aono, S. (1998) Heme environmental structure of CooA is modulated by the target dna binding, *J. Biol. Chem. 273*, 19988−19992.
22. Fox, J. D., He, Y. P., Shelver, D., Roberts, G. P., and Ludden, P. W. (1996) Characterization of the region encoding the CO-induced hydrogenase of *Rhodospirillum rubrum*, *J. Bacteriol. 178*, 6200−6208.
23. Rubtsov, I. V., Zhang, T., and Yoshihara, K. (2000) Development and application of a femtosecond time-resolved mid-infrared transient absorption spectrometer, *J. Spectrosc. Soc. Jpn. 49*, 292.
24. The dynamics were fitted using the following expression for global fitting: $a \times \exp[-(\lambda - \lambda')^2/w^2] \times (\exp[-(t - t_0)/\tau_2] + r_0)$, where $\lambda' = \lambda_0 + \Delta\lambda \times \exp[-(t - t_0)/\tau_1]$ and a, t_0, τ_1, τ_2, r_0, λ_0, and $\Delta\lambda$ are fitting parameters and t and λ stand for time and wavelength, respectively.
25. Hill, J. R., Dlott, D. D., Rella, C. W., Peterson, K. A., Decatur, S. M., Boxer, S. G., and Fayer, M. D. (1996) Vibrational dynamics of carbon monoxide at the active sites of mutant heme proteins, *J. Phys. Chem. 100*, 12100−12107.
26. Decatur, S. M., Depillis, G. D., and Boxer, S. G. (1996) Modulation of protein function by exogenous ligands in protein cavities: CO binding to a myoglobin cavity mutant containing unnatural proximal ligands, *Biochemistry 35*, 3925−3932.
27. Li, T. S., Quillin, M. L., Phillips, G. N., and Olson, J. S. (1994) Structural determinants of the stretching frequency of CO bound to myoglobin, *Biochemistry 33*, 1433−1446.
28. Li, X. Y., and Spiro, T. G. (1988) Is bound CO linear or bent in heme-proteins: Evidence from resonance Raman and infrared spectroscopic data, *J. Am. Chem. Soc. 110*, 6024−6033.
29. Phillips, G. N., Teodoro, M. L., Li, T. S., Smith, B., and Olson, J. S. (1999) Bound CO is a molecular probe of electrostatic potential in the distal pocket of myoglobin, *J. Phys. Chem. B 103*, 8817−8829.
30. Ray, G. B., Li, X. Y., Ibers, J. A., Sessler, J. L., and Spiro, T. G. (1994) How far can proteins bend the FeCO unit − distal polar and steric effects in heme-proteins and models, *J. Am. Chem. Soc. 116*, 162−176.
31. Vogel, K. M., Kozlowski, P. M., Zgierski, M. Z., and Spiro, T. G. (2000) Role of the axial ligand in heme-CO back-bonding: DFT analysis of vibrational data, *Inorg. Chim. Acta 297*, 11−17.
32. Vogel, K. M., Spiro, T. G., Shelver, D., Thorsteinsson, M. V., and Roberts, G. P. (1999) Resonance Raman evidence for a novel charge relay activation mechanism of the CO-dependent heme protein transcription factor CooA, *Biochemistry 38*, 2679−2687.
33. Uchida, T., Ishikawa, H., Takahashi, S., Ishimori, K., Morishima, I., Nakajima, H., and Aono, S. Unpublished results.
34. There could be another possible combination for the frequencies, i.e., 522 and 1973 cm^{-1} for point I and 491 and 1958 cm^{-1} for point II. However, it is inconsistent with the electron back-donation model and the available data set of heme proteins and model systems with heme changing between 5-c and 6-c forms. This combination of frequencies is not consistent with the proportion of 5-c and 6-c species in the sample, inferred from steady-state UV−vis absorption, IR absorption, and Raman spectroscopy.
35. Cao, W. X., Ye, X., Georgiev, G. Y., Berezhna, S., Sjodin, T., Demidov, A. A., Wang, W., Sage, J. T., and Champion, P. M. (2004) Proximal and distal influences on ligand binding kinetics in microperoxidase and heme model compounds, *Biochemistry 43*, 7017−7027.
36. Nishihara, Y., Sakakura, M., Kimura, Y., and Terazima, M. (2004) The escape process of carbon monoxide from myoglobin to solution at physiological temperature, *J. Am. Chem. Soc. 126*, 11877−11888.
37. Schotte, F., Lim, M. H., Jackson, T. A., Smirnov, A. V., Soman, J., Olson, J. S., Phillips, G. N., Wulff, M., and Anfinrud, P. A. (2003) Watching a protein as it functions with 150-ps time-resolved X-ray crystallography, *Science 300*, 1944−1947.
38. Champion, P. M. (1992) Raman and kinetic-studies of myoglobin structure and dynamics, *J. Raman Spectrosc. 23*, 557−567.
39. Steinbach, P. J., Ansari, A., Berendzen, J., Braunstein, D., Chu, K., Cowen, B. R., Ehrenstein, D., Frauenfelder, H., Johnson, J. B., Lamb, D. C., Luck, S., Mourant, J. R., Nienhaus, G. U., Ormos, P., Philipp, R., Xie, A. H., and Young, R. D. (1991) Ligand-binding to heme-proteins: Connection between dynamics and function, *Biochemistry 30*, 3988−4001.
40. Collman, J. P., and Fu, L. (1999) Synthetic models for hemoglobin and myoglobin, *Acc. Chem. Res. 32*, 455−463.
41. Kachalova, G. S., Popov, A. N., and Bartunik, H. D. (1999) A steric mechanism for inhibition of CO binding to heme proteins, *Science 284*, 473−476.
42. Roberts, G. P., Kerby, R. L., Youn, H., and Conrad, M. (2005) CooA, a paradigm for gas sensing regulatory proteins, *J. Inorg. Biochem. 99*, 280−292.
43. Thorsteinsson, M. V., Kerby, R. L., Conrad, M., Youn, H., Staples, C. R., Lanzilotta, W. N., Poulos, T. J., Serate, J., and Roberts, G. P. (2000) Characterization of variants altered at the N-terminal proline, a novel heme-axial ligand in CooA, the CO-sensing transcriptional activator, *J. Biol. Chem. 275*, 39332−39338.
44. Youn, H., Kerby, R. L., Thorsteinsson, M. V., Conrad, M., Staples, C. R., Serate, J., Beack, J., and Roberts, G. P. (2001) The heme pocket afforded by Gly(117) is crucial for proper heme ligation and activity of CooA, *J. Biol. Chem. 276*, 41603−41610.
45. Newmyer, S. L., Sun, J., Loehr, T. M., and Demontellano, P. R. O. (1996) Rescue of the horseradish peroxidase His-170 → Ala mutant activity by imidazole: Importance of proximal ligand tethering, *Biochemistry 35*, 12788−12795.
46. Depillis, G. D., Decatur, S. M., Barrick, D., and Boxer, S. G. (1994) Functional cavities in proteins: A general-method for proximal ligand substitution in myoglobin, *J. Am. Chem. Soc. 116*, 6981−6982.
47. Franzen, S. (2002) Carbonmonoxy rebinding kinetics in H93G myoglobin: Separation of proximal and distal side effects, *J. Phys. Chem. B 106*, 4533−4542.
48. Franzen, S., and Boxer, S. G. (1997) On the origin of heme absorption band shifts and associated protein structural relaxation in myoglobin following flash photolysis, *J. Biol. Chem. 272*, 9655−9660.

BI0603672